Available online at www.sciencedirect.com
ScienceDirect
Journal of Molecular Catalysis A: Chemical 274 (2007) 24–32
JOURNAL OF MOLECULAR CATALYSIS A: CHEMICAL
www.elsevier.com/locate/molcata

Shape-selective isopropylation of biphenyl over CIT-5 zeolites with CFI topology

Hiroyoshi Maekawa [a], Chikayo Naitoh [a], Kazunori Nakagawa [a], Akira Iida [a], Kenichi Komura [a], Yoshihiro Kubota [a,1], Yoshihiro Sugi [a,*], Jong-Ho Kim [b], Gon Seo [b]

[a] *Department of Materials Science and Technology, Faculty of Engineering, Gifu University, Gifu 501-1193, Japan*
[b] *School of Applied Chemical Engineering and The Research Institute for Catalysis, Chonnam National University, Gwangju 500-757, Republic of Korea*

Received 21 October 2006; received in revised form 10 April 2007; accepted 15 April 2007
Available online 19 April 2007

Abstract

In the isopropylation of biphenyl (BP) over a one-dimensional fourteen-membered ring (14-MR) CIT-5 zeolite with CFI topology, the selectivities for 4,4′-diisopropylbiphenyl (4,4′-DIPB) were 50–70% in the bulk and encapsulated products at moderate temperatures below 300 °C. However, they decreased at high temperatures such as 350 °C. These results mean that CIT-5 zeolites can preferentially exclude the transition state of the bulky DIPB isomers from their channels, thus resulting in the selective formation of 4,4′-DIPB. However, the isomerization of 4,4′-DIPB occurred on external and internal acid sites of the zeolite.

Keywords: CIT-5 zeolite; CFI topology; Isopropylation; Biphenyl; 4,4′-Diisopropylbiphenyl; Shape-selectivity

1. Introduction

The shape-selective alkylation of polynuclear aromatics is interesting for the synthesis of advanced materials such as liquid crystalline and heat-resistant polymers [1–18]. We had previously found that H-mordenite (MOR) was an excellent catalyst for the shape-selective isopropylation of biphenyl (BP), and concluded that the shape-selective catalysis for the formation of 4,4′-diisopropylbiphenyl (4,4′-DIPB) was due to the effective exclusion of the transition state of the bulky isomers from the MOR channels [1–6]. The extent of the exclusion should be influenced by the type of zeolites. It is interesting to note that the structure of the zeolites is related to the shape-selective catalysis. Recently, we have described the isopropylation of BP over twelve-membered ring (12-MR) molecular sieves: H-[Al]-SSZ-24 [12,13], SAPO-5 [14], MAPO-5 (M: Mg, Ca, Sr, Ba, and Zn) [15–17], and SSZ-31 [18], which have larger pore entrances than MOR. We found that the selectivities for 4,4′-DIPB over these zeolites are lower than that over H-MOR. Such differences in the selectivity for 4,4′-DIPB are due to the less effective exclusion of the bulky transition states from their channels.

Recently, CIT-5 zeolite (topology: CFI), which has one-dimensional fourteen-membered ring (14-MR) pore-entrances (0.72 nm × 0.75 nm) with slightly corrugated channels (16-MR cage) [19] was synthesized by using *N*(16)-methylsparteinium ($MeSPA^+$) as the structure directing agent (SDA) [20–22]. It is interesting to establish how CIT-5 zeolite works for acid catalysis. The question has encouraged us to investigate the catalytic properties of CIT-5 zeolite. In this paper, we describe the shape-selective isopropylation of BP over CIT-5 zeolite, and compared it with the catalytic properties of other 12-MR and 14-MR zeolites.

2. Experimental

2.1. Catalysts

CIT-5 zeolites were synthesized according to our previous work [22]. Typical procedures for the synthesis from highly dealuminated H-Y zeolite as silica source are as follows. The gel composition was in the ratio: SiO_2:[$MeSPA^+$]

* Corresponding author.
E-mail address: sugi@apchem.gifu-u.ac.jp (Y. Sugi).
[1] Present address: Department of Materials Science and Engineering, Graduate School of Engineering, Yokohama National University, Yokohama 240-8501, Japan.

1381-1169/$ – see front matter © 2007 Elsevier B.V. All rights reserved.
doi:10.1016/j.molcata.2007.04.014

Table 1
The synthetic condition and properties of CIT-5 zeolite[a]

Zeolite[a]	Silica source	Synthetic condition			Average particle size (μm)	SiO_2/Al_2O_3	Surface area (m^2/g)	External surface area (m^2/g)[b]	Pore volume (mm^3/g)	NH_3 peak temp. (°C)	Acid amount (mmol/g)
		Temp. (°C)	Time (day)	Rotation (rpm)							
CFI-I	Fumed silica[c]	175	8	0	45 × 10	286	156	21	69	228	0.003
CFI-II	Fumed silica[c]	150	10	66	2.0 × 0.2	262	295	60	117	281	0.062
CFI-III	HY[d]	150	10	66	1.0 × 0.3	160	339	38	141	294	0.129

[a] Gel composition: SiO_2:$MeSPA^+OH^-$:LiOH:$Al(NO_3)_3$:H_2O = 1:0.2:0.1:0.005:50.
[b] Calculated from *t*-plot of N_2 adsorption.
[c] Cab-O-Sil M5.
[d] Tosoh HSZ-390HUA (SiO_2/Al_2O_3 = 380).

OH^-:LiOH:$Al(NO_3)_3$:H_2O = 1.0:0.2:0.1:0.005:50. The synthesis gel was prepared by mixing $Al(NO_3)_3 \cdot 9H_2O$ (0.094 g), $[MeSPA^+]OH^-$ solution (0.565 mmol/g, 17.71 g), $LiOH \cdot H_2O$ (0.208 g), dealuminated H-Y (FAU) zeolite (3.016 g; HSZ-390HUA (SiO_2/Al_2O_3 = 380); Tosoh Corporation, Tokyo, Japan), and deionized water (29.6 g). The gel was taken into a 125-ml Teflon insert, and placed in a stainless steel Parr autoclave. The autoclave was heated at 150 °C for 10 days at a rotation of 66 rpm. After cooling to ambient temperature, the crystals thus obtained were filtered, washed several times with deionized water, and dried overnight.

The resulting as-synthesized CIT-5 sample was calcined to its lithium form at 700 °C for 6 h in a flow of air (100 ml/min). The lithium form CIT-5 sample (3.04 g) was then transformed to its NH_4 form by using NH_4NO_3 (6.08 g) in 300 ml of water at 100 °C for 24 h in a 500-ml polypropylene bottle. After cooling to ambient temperature, the zeolite was filtered, and washed well with deionized water. This process was repeated twice. Finally, NH_4-form CIT-5 zeolite was calcined at 550 °C for 6 h to the H-form of CIT-5 zeolite.

The conditions and properties of CIT-5 zeolites used in this study are shown in Table 1.

H-Beta zeolite (BEA) was synthesized according to the procedure in the literature [23]. H-Mordenite (MOR) zeolite was obtained from Tosoh Corporation, Tokyo, Japan (HSZ-690HOA) (SiO_2/Al_2O_3 = 206).

2.2. Isopropylation of BP

The isopropylation of BP was carried out in a 100 ml SUS-316 autoclave under propene pressure. Typical reaction conditions were: BP 50 mmol, catalyst 0.25 g, reaction temperature 150–250 °C, and 4 h under a propene pressure of 0.8 MPa. An autoclave containing BP and catalyst was purged with nitrogen. The autoclave was then heated to the reaction temperature, propene was introduced to the autoclave, and the reaction was started by agitation. The propene pressure was maintained constant throughout the reaction. After cooling, the autoclave to ambient temperature, the catalyst was filtered off, and the liquid products were analyzed by a GC-14A gas chromatograph (Shimadzu Corp., Kyoto, Japan) equipped with an Ultra-1 capillary column (25 m × 0.2 mm; Agilent Technologies Inc., MA, USA). The products were also identified by a Shimadzu GC–MS 5000 gas chromatograph–mass spectrometer. The yield of each product was calculated on the basis of the amounts of starting BP, and the selectivity for each isopropylbiphenyl (IPBP) and diisopropylbiphenyl (DIPB) isomers were expressed on the basis of the total amounts of IPBP and DIPB isomers, respectively.

$$\text{Selectivity for a DIPB (IPBP) isomer (\%)} = \frac{\text{Each DIPB(IPBP) isomer (mol)}}{\text{DIPB (IPBP) isomers (mol)}} \times 100$$

The analysis of the encapsulated products in the catalyst used for the reaction was carried out as follows. The catalyst was separated by filtration, washed well with 200 ml of acetone, and dried at 110 °C for 12 h. Hundred milligram of the resulting catalyst was carefully dissolved using 3 ml of aqueous hydrofluoric acid (47%) at room temperature. This solution was neutralized with solid potassium carbonate, and the organic layer was extracted three times with 20 ml of dichloromethane. After removal of the solvent *in vacuo*, the residue was dissolved in 5 ml of toluene, and the resulting samples were then analyzed according to the procedure that has been used for the bulk products.

2.3. Characterization of the catalysts

The crystal structures of the zeolites were determined by powder X-ray diffraction (XRD) using a Shimadzu XRD-6000 diffractometer with Cu Kα radiation (λ = 1.5418 Å). Elemental analysis was performed by inductive coupled plasma atomic emission spectroscopy on a JICP-PS-1000 UV spectrometer (Teledyne Leeman Labs, Inc., NH, USA). The crystal size and morphology of the zeolites were determined by an S-4300 FE-SEM microscope (Hitachi Corp., Tokyo, Japan). Nitrogen adsorption measurements were carried out on a Belsorp 28SA apparatus (Bel Japan Inc., Osaka, Japan). Adsorption of *o*-xylene was measured by gravimetry using a quartz spring balance at 120 °C after the evacuation of the zeolite at 500 °C. Ammonia temperature programmed desorption (NH_3-TPD) was measured using a Bel TPD-66 apparatus: the zeolite was evacuated at 400 °C for 1 h, and ammonia was adsorbed at 100 °C followed by further evacuation for 1 h. The sample was then heated from 100 to 710 °C at a rate of 10 °C/min in a helium stream. The ^{27}Al NMR spectra were recorded at ambient temperature under magic angle spinning (MAS) by using 7.0 mm zirconia rotors

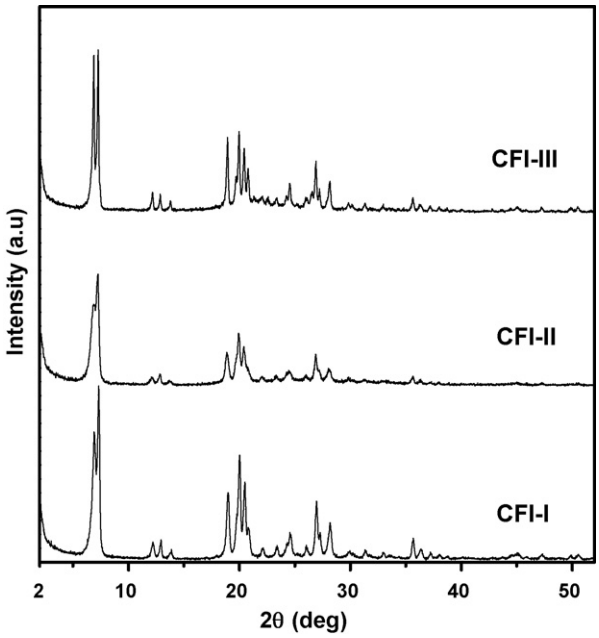

Fig. 1. XRD patterns of calcined CIT-5 zeolites.

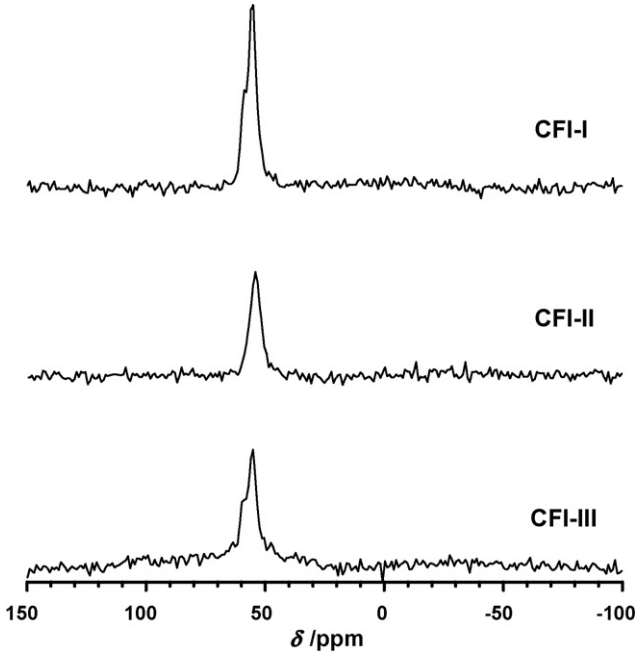

Fig. 3. ^{27}Al MAS NMR spectra of H-form samples of (a) CFI-I, (b) CFI-II and (c) CFI-III.

with a spinning rate of 4 kHz on an Inova 400 spectrometer (Varian Corp., MA, USA). Thermogravimetric (TG) analysis was performed on a Shimadzu DTG-50 analyzer with temperature-programmed rate of 10 °C min^{-1} in an air stream.

3. Results and discussion

3.1. Properties of CIT-5 zeolite

Typical synthesis conditions for CIT-5 zeolites and their physico-chemical properties related to catalysis are shown in Table 1. The XRD patterns of the calcined CIT-5 zeolites and the SEM images of the as-synthesized CIT-5 zeolites are shown in Figs. 1 and 2, respectively. CIT-5 zeolites have needle or plate morphologies. CFI-I, prepared under static conditions by using fumed silica, has a plate morphology with size of 45 μm × 10 μm. CFI-II, prepared from fumed silica with the rotation of the reaction vessel, has relatively broad XRD patterns. It has small needle crystals with an average size of less than 2 μm × 0.2 μm. CFI-III, prepared from highly dealuminated H-Y (FAU) zeolites with the rotation, is small needles of sizes of 1.0 μm × 0.3 μm. These results indicate that CFI-II and CFI-III have similar particle sizes. The SiO_2/Al_2O_3 ratios of the CIT-5 zeolites were 286, 262, and 160, respectively. CFI-III has the lowest SiO_2/Al_2O_3 ratio among the CIT-5 zeolites.

^{27}Al MAS NMR spectra of the proton forms of CFI-I, CFI-II, and CFI-III are shown in Fig. 3. All ^{27}Al spectra have single peaks at around 50 ppm, which are assigned to the tetrahedral Al^{3+} species. However, there was no peak assigned to the octahedral Al^{3+} species in these zeolites. These results indicate that the Al^{3+} species are incorporated in the zeolite framework in all CIT-5 zeolites. The tetrahedral aluminum works for the acid sites in acid catalysis.

Nitrogen adsorption isotherms of CIT-5 zeolites are typically of type I as shown in Fig. 4. The amounts of N_2 adsorption on CFI-II and CFI-III were almost the same. However, the amount on CFI-I was considerably lower than that on CFI-II and CFI-

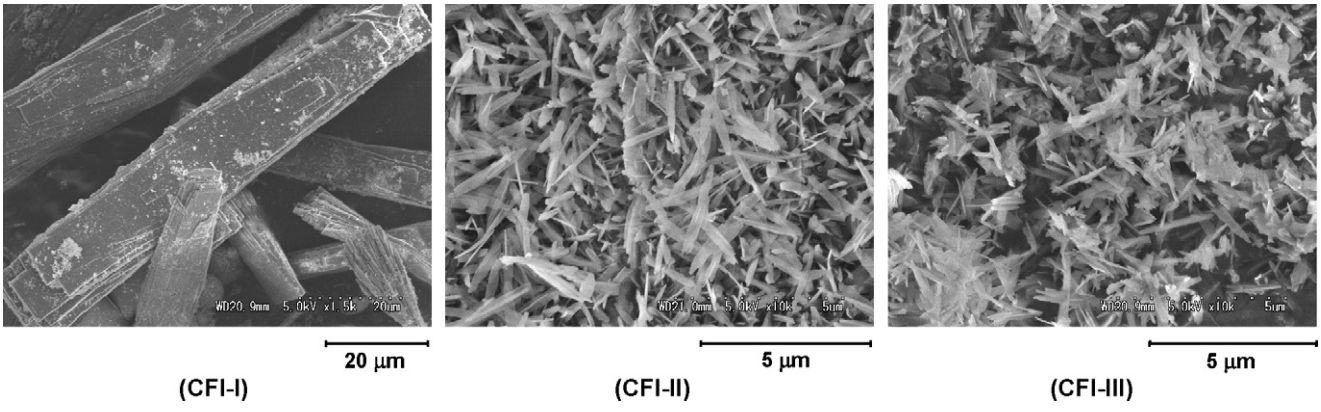

Fig. 2. SEM images of as-synthesized CIT-5 zeolites.

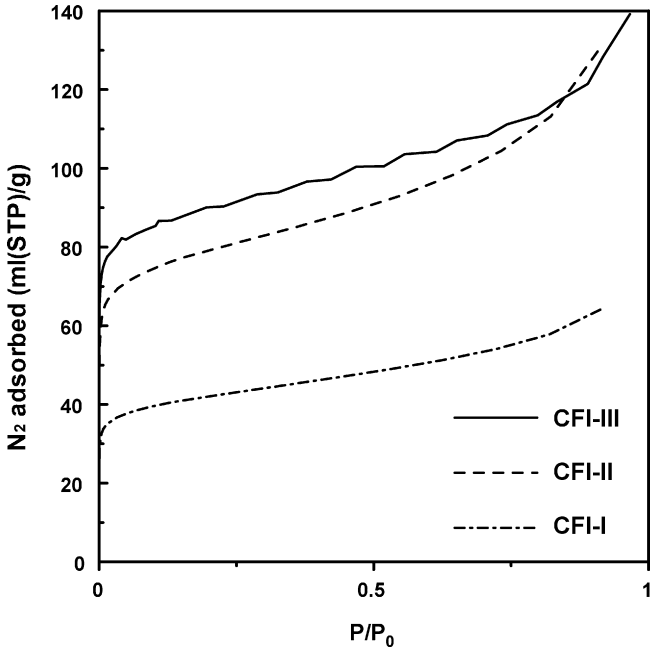

Fig. 4. N_2 adsorption isotherms of CIT-5 zeolites used for the catalytic reactions.

III. The surface areas of the CIT-5 zeolites calculated from N_2 adsorption were 156, 295, and 339 for CFI-I, CFI-II, and CFI-III, respectively. Their external surface areas calculated from the *t*-plot of N_2 adsorption were 21, 60, and 38, respectively. The pore volume of CFI-1 was much lower than those of CFI-II and CFI-III.

Fig. 5 shows the adsorption of *o*-xylene on CIT-5 zeolites. The adsorption of *o*-xylene was rapidly saturated on all zeolites. However, the saturation of *o*-xylene adsorption depends on the particle size in the order: CFI-I ≪ CFI-III < CFI-II.

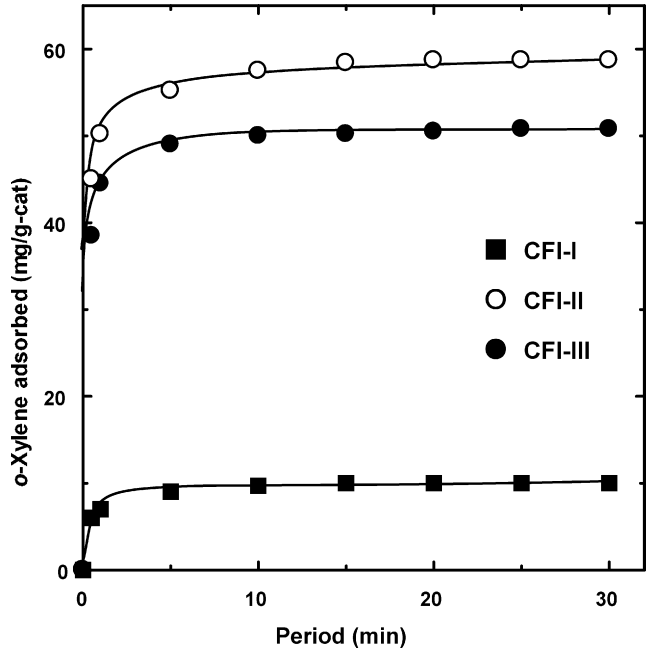

Fig. 5. *o*-Xylene adsorption on CIT-5 zeolites used for the catalytic reactions. Adsorption conditions—Sample: 0.1 g; temperature: 120 °C.

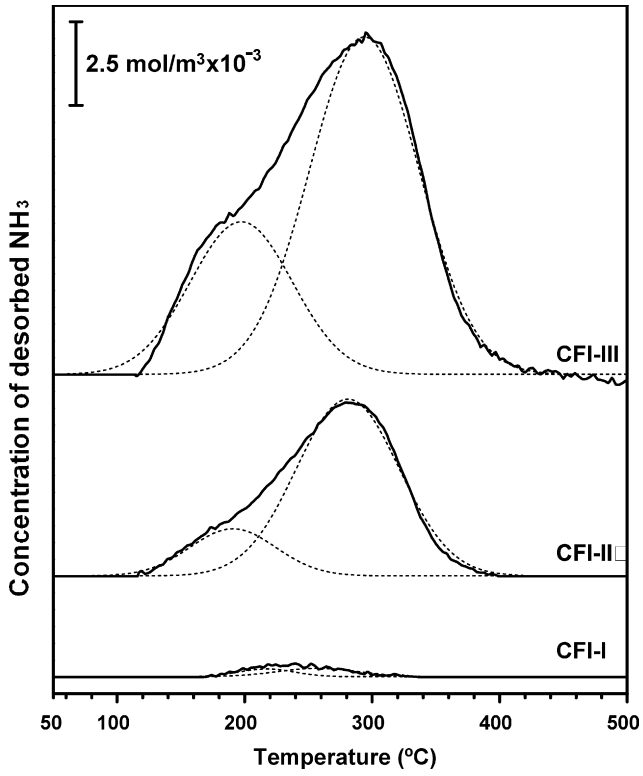

Fig. 6. NH_3-TPD profiles of CIT-5 zeolites used for the catalytic reactions.

The NH_3-TPD profiles were shown in Fig. 6. They show that the amounts of NH_3 desorbed reflect the amounts of acid sites in the order: CFI-III > CFI-II ≫ CFI-I, and that the peak temperature of the NH_3 desorption was increased in the order: CFI-I ≪ CFI-II < CFI-III. These results indicate that CFI-III has the highest acidity. These acidities of CIT-5 zeolites, particularly CFI-II and CFI-III, are strong enough for the isopropylation of BP. On the other hand, the amount of acid sites on CFI-I is much lower although CFI-I has a SiO_2/Al_2O_3 ratio comparable to that of CFI-II.

Judging from their physico-chemical properties, CFI-II and CFI-III are typical microporous materials with high surface area and acidity. However, the adsorption of N_2 and *o*-xylene, and the amounts of acid on CFI-I are unusually low compared to the values for CFI-II and CFI-III, although the almost identical XRD patterns and the incorporation of aluminum in their frameworks was observed for all the CIT-5 zeolites. CFI-I also has a much smaller surface area and pore volume than CFI-II and CFI-III. These results suggest that CFI-I has blockages inside the crystals because the internal surface area and pore volume of the zeolites should be independent of their particle size. The blockages, possibly by disorder in the large crystals, reduce the accessible volumes, resulting in the prevention of the adsorption of N_2, *o*-xylene, and NH_3. However, further research is necessary in order to understand the details of the blockage of CFI-I.

3.2. The influence of particle size on the isopropylation

Table 2 shows the influence of the particle size on the isopropylation of BP over CIT-5 zeolites prepared by

Table 2
The isopropylation of BP over CIT-5 zeolites[a]

Run	Catalyst	SiO_2/Al_2O_3	Period (h)	Conv. (%)	Product distribution (%)			Selectivity for 4,4′-DIPB (%)
					IPBP	DIPB	TriIPB	
1	CFI-I	286	4	5	94	6	–	73
2	CFI-II	262	4	85	28	58	12	58
3	CFI-III	160	4	88	28	65	6	54
4	MOR	206	4	73	33	64	–	87
5	BEA	110	4	60	65	30	5	24
6	FAU	380	4	20	86	14	–	5

[a] Reaction conditions: BP, 50–200 mmol; Catalyst, 0.250–1.0 g (BP/catalyst = 200 mmol/g); temperature, 250 °C; period, 4 h.

different synthetic methods. The isopropylation gave IPBP and DIPB isomers, preferentially. Triisopropylbiphenyl (TriIPB) isomers were also observed at higher temperatures. The activities depended strongly on the particle size of the CIT-5 zeolites. The activity of CFI-I with the largest particle size was the lowest among the CIT-5 zeolites (run 1). This was due to the small amounts of acid sites participating in the catalysis because of the blockage of the channels, as discussed above. The number of pore entrances and the low diffusivity of the reactants and products in the large crystals also caused the low activity of the CFI-I. On the other hand, CFI-II and CFI-III had a small particle size but much higher activities (runs 2 and 3). They gave moderate yields of the DIPB isomers. Small particles such as CFI-II and CFI-III have many opportunities for the reactants to enter the pores, resulting in high level of the activity. These differences in catalytic activity were also supported by the differences in N_2, *o*-xylene, and NH_3 adsorption among the CIT-5 zeolites.

The selectivities for 4,4′-DIPB over CIT-5 zeolites are at the level of 50–70%. These results indicate that CIT-5 zeolites are shape-selective in the isopropylation of BP. CIT-5 zeolites can exclude the transition state of the bulky DIPB isomers by steric restriction in their channels resulting in the preferential formation of the least bulky 4,4′-DIPB. CFI-I has the highest selectivity for 4,4′-DIPB among the CIT-5 zeolites, however, the selectivities over CFI-II and CFI-III at 250 °C were 54–58%. These lower selectivities over CFI-II and CFI-III may be due to the isomerization of 4,4′-DIPB at their external acid sites because small particles have a high external surface area as well as large numbers of pore entrances compared to the large particles. The highest selectivity for 4,4′-DIPB obtained for CFI-I indicates the shape-selectivity of the CFI channels because the isomerization of 4,4′-DIPB is not so extensive at their external acid sites.

TG profiles of the zeolites used for the isopropylation have two types of peaks for all catalysts: 250–450 °C assigned to the encapsulated products and 450–750 °C to the coke deposited on the CIT-5 zeolites (data not shown). The amounts of coke deposited on CFI-II and CFI-III were 4.5 and 5.3%, respectively, calculated from the weight loss in the TG profiles. These results suggest that coke formation on the CIT-5 zeolites, CFI-II and CFI-III, is not severe enough to retard the isopropylation: this is due to small amounts of acid sites in these zeolites. Similar phenomena were observed in the isopropylation over highly dealuminated H-MOR [1–6]. On the other hand, the carbon deposit on CFI-I was almost negligible: this corresponds to low activity due to the participation of only small numbers of acid sites in the catalysis because of blockage of the channels as discussed above.

The results of the isopropylation of BP over some typical high-silica large-pore zeolites are also shown in Table 2. Only MOR exhibits high catalytic activity and selectivity for 4,4′-DIPB as previously described [1–6]. However, the BEA and FAU zeolites exhibited low selectivities for 4,4′-DIPB (runs 5 and 6). These results are due to the large reaction space in their channels for the discrimination of the slimmest isomer from other isomers. The selectivity for 4,4′-DIPB over CIT-5 zeolite was lower than that over MOR zeolite. This means that the steric restriction of the DIPB isomers by the CIT-5 channels is less severe than that for the MOR channels resulting in lower selectivity.

Among the three types of CIT-5 zeolite, CFI-III was chosen as the catalyst for further research because it has the lowest SiO_2/Al_2O_3 ratio and the highest surface area with small particle size, and moderate catalytic activity for the isopropylation of BP.

3.3. The influence of reaction temperature on the isopropylation of BP

Fig. 7 shows the influence of the reaction temperature on the yield of isopropylates in the isopropylation of BP. The conversion of BP increased with increasing reaction temperatures. The IPBP isomers produced preferentially at low temperatures. The increase in the reaction temperature enhanced the yield of DIPB isomers accompanying the decrease in the yield of IPBP isomers, and finally the TriIPB isomers increased at high temperature with the decrease in the yield of DIPB isomers. These results show the typical consecutive reaction mechanism: BP to IPBP, IPBP to DIPB, and DIPB to TriIPB. The CIT-5 channels are sufficiently wide to allow the formation of the bulky TriIPB isomers. The accumulation of TriIPB isomers was observed in the encapsulated products, particularly, at high temperatures, because of their low diffusion in the channels (data not shown). These results are different from the isopropylation of BP over MOR zeolites: the MOR channels exclude the formation of TriIPB isomers [1–6].

Fig. 8 shows the influence of the reaction temperatures on the selectivity for DIPB isomers in the isopropylation of BP. The selectivities for 4,4′-DIPB were 50–60% up to 300 °C, whereas, they decreased at higher temperatures, such as 350 °C. The selec-

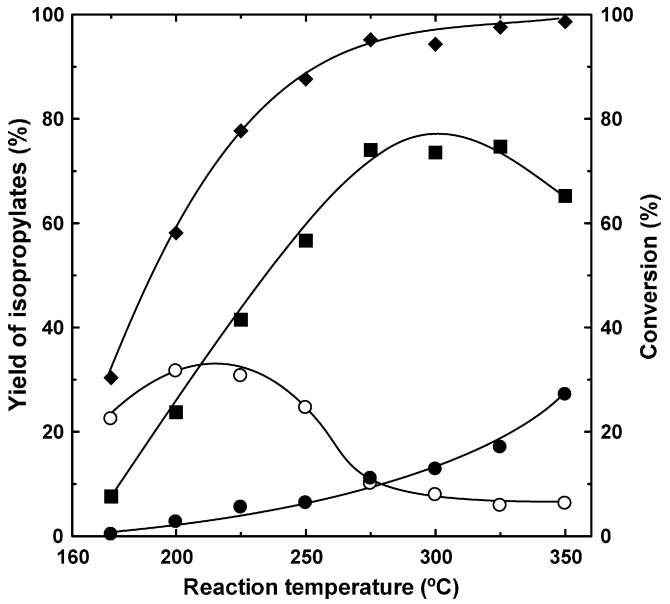

Fig. 7. The influence of reaction temperature on the yield of isopropylates in the isopropylation of BP over the CIT-5 zeolite. Reaction conditions—BP: 50 mmol; catalyst: CFI-III, 250 mg; temperature: 175–350 °C; pressure of propene: 0.8 MPa; period: 4 h. Legends: (◆) conversion. Yield of isopropylates: (◯) IPBP; (■) DIPB; (●) TriIPB.

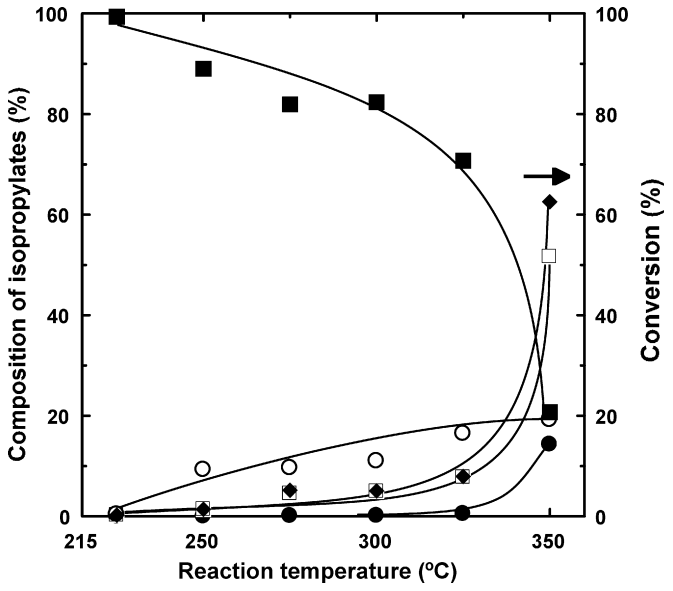

Fig. 9. The influence of reaction temperature on the isopropylation of 4,4′-DIPB over CIT-5 zeolite. Reaction conditions: 4,4′-DIPB, 25 mmol; catalyst: CFI-III, 250 mg; temperature: 175–350 °C; pressure of propene: 0.8 MPa; period: 4 h. Legends: (◆) Conversion; (■) 4,4′-DIPB; (●) yield of IPBP; (□) yield of DIPB isomers isomerized from 4,4′-DIPB; (◯) yield of TriIPB.

tivity for 4,4′-DIPB in the encapsulated products was also at a similar level to that of the bulk products. It decreased gradually with increasing reaction temperature below 300 °C. However, it decreased rapidly to 30% at 350 °C. These results show that the formation of 4,4′-DIPB occurred due to the shape-selective catalysis inside the channels of the CIT-5 zeolites at moderate temperatures below 300 °C. The channels of the CIT-5 zeolites are small enough to exclude the formation of the bulky DIPB isomers, thus resulting in the shape-selective formation of 4,4′-DIPB. The decrease in the selectivity for 4,4′-DIPB in the bulk and encapsulated products at high temperatures is due to the isomerization of the 4,4′-DIPB. The isomerization of 4,4′-DIPB occurs on the external and internal acid sites. However, it is also possible that the increase in temperature lowers the possibility of the "restricted transition state selectivity", thus resulting in the decrease of the selectivity for 4,4′-DIPB. The isomerization of 4,4′-DIPB over the CIT-5 zeolites is quite different from the isopropylation of BP over MOR. However, a similar isomerization of 4,4′-DIPB was observed in the isopropylation of BP over SSZ-24 and MAPO-5 with AFI topology [16–20].

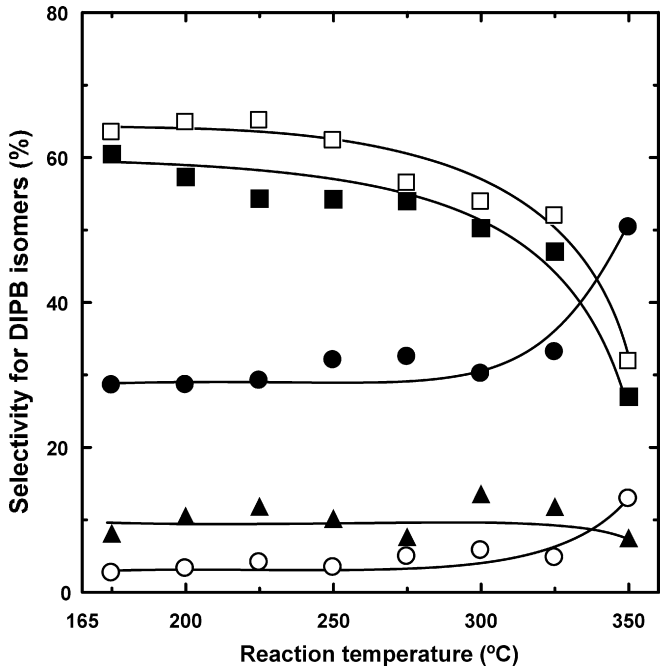

Fig. 8. The influence of reaction temperature on the selectivity for DIPB isomers in the isopropylation of BP over the CIT-5 zeolite. Reaction conditions: *see* in Fig. 7. Legends: selectivity in the bulk products: (■) 4,4′-DIPB; (●) 3,4′-DIPB; (◯) 3,3′-DIPB; (▲) 2,*x*′-DIPB. (□) selectivity for 4,4′-DIPB in the encapsulated products.

3.4. The influence of the reaction temperature on the isomerization of 4,4′-DIPB

The isopropylation of 4,4′-DIPB under propene pressure was examined to elcuidate the reactivity of 4,4′-DIPB as shown in Fig. 9. TriIPB isomers formed by the isopropylation of 4,4′-DIPB were observed in small amounts even at 250 °C, and increased with increasing temperatures to 20% at 350 °C. Small amounts of IPBP isomers formed by the de-alkylation of 4,4′-DIPB were found below 325 °C, however, they increased to 15% at 350 °C. Small amounts of 3,4′-and 3,3′-DIPB formed from 4,4′-DIPB were obtained below 300 °C, however, their formation was enhanced at 350 °C. These results mean that the extensive isomerization of 4,4′-DIPB occurred at 350 °C, and was accompanied by an increase in the formation of the IPBP and TriIPB isomers. TriIPB isomers were accumulated particularly in the encapsulated products (data not shown).

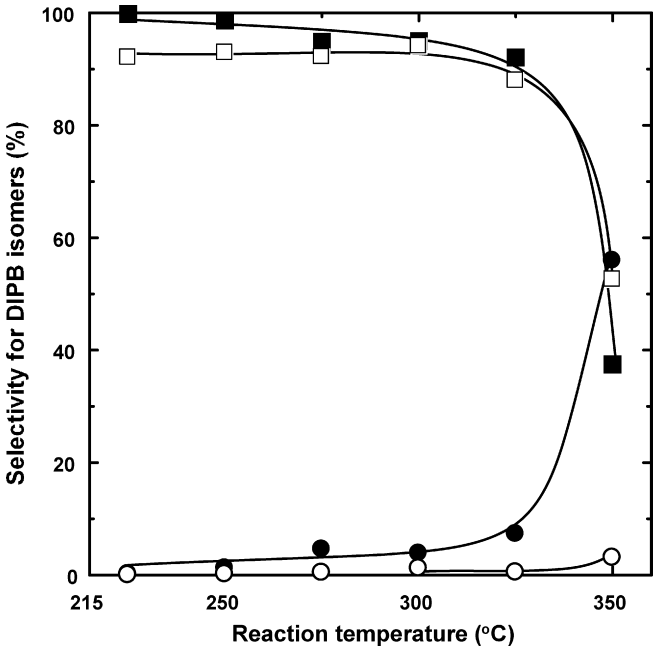

Fig. 10. The influence of reaction temperature on the selectivity for DIPB isomers in the isopropylation of 4,4′-DIPB over the CIT-5 zeolite. Reaction conditions: see Fig. 9. Legends: see Fig. 8.

Fig. 10 shows the influence of the reaction temperature on the selectivity for 4,4′-DIPB in the isopropylation of 4,4′-DIPB. Isomerization of 4,4′-DIPB was not extensively observed below 300 °C, however, the decreases in the selectivity for 4,4′-DIPB by the isomerization of 4,4′-DIPB were observed in both the bulk and the encapsulated products at temperatures of 325 and 350 °C. These results show that the isomerization of 4,4′-DIPB occurs on the external and internal acid sites at high temperatures, and that the CIT-5 channels are large enough for the formation of the bulky TriIPB isomers. This is quite similar to the features of the isopropylation of BP discussed above.

3.5. The influence of the amount of catalyst on the isopropylation of BP

It is interesting to elucidate the influence of the amount of acids on the selectivity for 4,4′-DIPB in the isopropylation of BP because numbers of the external acid sites are related to the amounts of catalyst. Fig. 11 shows the influence of the amount of catalyst on the selectivity for DIPB isomers at 300 °C. The selectivities for 4,4′-DIPB in the bulk products was gradually decreased with increasing in amounts of catalyst against BP, however, the selectivities for 4,4′-DIPB in the encapsulated products was not significantly changed with the increase in the amounts of catalyst. These decreases in the selectivity by using large amount of catalyst are due to the isomerization of 4,4′-DIPB at the external acid sites because of the increase in the external acid sites, however, the isomerization of 4,4′-DIPB inside the channels is not extensive at 300 °C. These results show that the isomerization of 4,4′-DIPB gradually occurs at external acid sites even at 300 °C in the isopropylation of BP.

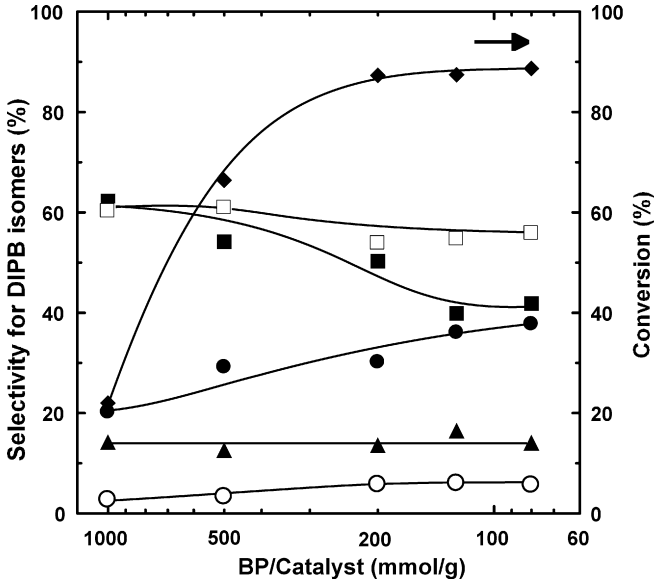

Fig. 11. The influence of catalyst amount on the selectivity for DIPB isomers in the isopropylation of BP over the CIT-5 zeolite. Reaction conditions: BP: 8–50 mmol; catalyst: CFI-III, 100 mg; temperature: 300 °C; propene pressure: 0.8 MPa; period: 4 h. Legends: see Fig. 8.

3.6. Mechanistic aspects of the catalysis over CIT-5 zeolite

CIT-5 zeolite has one-dimensional 14-MR pore entrances (0.72 nm × 0.75 nm) with slightly corrugated channels (16-MR cage). Their channels are sufficiently small for the shape-selective isopropylation of BP, and they can differentiate the transition state to form 4,4′-DIPB from other bulky DIPB isomers, thus resulting in the selective formation of the least bulky 4,4′-DIPB.

Other 14-MR zeolites, UTD-1 zeolite, which has a pore entrance of 0.74 nm × 0.95 nm with straight channels (topology: DON) [24] and SSZ-53 zeolite, which has a pore entrance of 0.65 nm × 0.88 nm with corrugated channels (topology: SFH) [25], gave principally DIPB isomers with 2-isopropyl group (2,*x*′-DIPB; 2,2′- and 2,3′-, and 2,4′-DIPB), and the selectivities for 4,4′-DIPB were as low as 10–15%. These zeolites had no shape-selective natures in the isopropylation of BP [12,26]. These differences are due to the differences in their structures, particularly the pore entrance and the reaction space. The reaction space of CIT-5 zeolite is small enough for the discrimination of 4,4′-DIPB from the other isomers. However, the isopropylation of BP over UTD-1 and SSZ-53 zeolites is governed kinetically or thermodynamically because these channels are too wide to discriminate the transition state to form 4,4′-DIPB from those of other isomers.

CIT-5 zeolite had a lower selectivity for 4,4′-DIPB even at lower temperatures than MOR zeolite, which has the highest selectivity among the zeolites. This may be due to the difference in the reaction space in the channels because CIT-5 has larger channels than MOR. The exclusion of the bulky 3,4′-DIPB should be stricter for MOR than for CIT-5 zeolite, and the formation of bulkier 3,4′-DIPB was not completely excluded.

We have also found the selectivities for 4,4′-DIPB were 60–70% in the isopropylation of BP over several one-dimensional 12-MR zeolites with straight channels: SSZ-24 [12,13], SAPO-5 [14], MAPO-5 (M: Mg, Ca, Sr, Ba, and Zn) [15–17] whose pore entrances are 0.73 nm × 0.73 nm with AFI topology, and SSZ-31 (0.56 nm × 0.82 nm) [18]. The selectivity for 4,4′-DIPB decreased in the order: MOR > SSZ-24, MAPO-5 (M: Mg, Ca, Sr, Ba, and Zn), and SAPO-5 ≈ SSZ-31 > CIT-5 ≫ UTD-1. This order corresponds to the order of the size of the pore entrances. These differences in the selectivity for 4,4′-DIPB by the types of zeolites suggest the importance of the channel width on the shape-selective catalysis. These results for the 12-MR and 14-MR zeolites suggest that the zeolites with straight channels have "restricted transition state selectivity", and that the selectivity is controlled by the exclusion of the bulky isomers at the transition state from the channels. In addition to "restricted transition state selectivity", "reactant selectivity" also operates in the selective formation of 4,4′-DIPB. However, we consider that "the products selectivity" does not operate much in our catalysis because the selective formation of 4,4′-DIPB is due to the slow isomerization inside the channels as discussed in the above section.

The selectivities for 4,4′-DIPB in the bulk and encapsulated DIPB isomers decreased at higher temperatures (325–350 °C) in the isopropylation of BP over CIT-5 zeolite as shown in Fig. 8. The decrease in the selectivities for 4,4′-DIPB in both the bulk and encapsulated products was also observed in the isopropylation of 4,4′-DIPB under propene pressure. These results show that the decrease in the selectivity is due to the isomerization of 4,4′-DIPB. Both the internal and external acid sites should participate in the isomerization. The decrease in the selectivity for 4,4′-DIPB in the bulk products was also observed even at 300 °C by the increase in the amount of catalyst although the selectivity for 4,4′-DIPB in the encapsulated products was not significantly changed. These results show that the isomerization of 4,4′-DIPB inside the channels is not extensive at 300 °C, although 4,4′-DIPB is gradually isomerized at the external acid sites. The isomerization of 4,4′-DIPB at high temperatures suggests that the channels of CIT-5 zeolite are large enough to allow the isomerization of 4,4′-DIPB although they are shape-selective for the formation of 4,4′-DIPB. It is also possible due to the decrease in the steric restriction of the CIT-5 channels at the transition states of DIPB isomers, thus resulting in the isomerization of 4,4′-DIPB to bulky and thermodynamically stable 3,4′-DIPB.

These features of the CIT-5 zeolite are quite different from those of H-MOR: no isomerization occurred inside the MOR channels because of the steric restriction. However, a similar isomerization of 4,4′-DIPB in the encapsulated products occurred for SSZ-24 [12,13] and MAPO-5 (M: Mg, Zn) [15–17] with AFI topology.

The TriIPB isomers by the isopropylation of 4,4′-DIPB as well as 3,4′-DIPB by the isomerization of 4,4′-DIPB were found in the encapsulated products, particularly, at the high temperatures. These results show that CIT-5 channels are large enough to allow the formation of the bulky TriIPB isomers although they are small enough for the selective formation of 4,4′-DIPB in the isopropylation of BP.

The particle size of the CIT-5 zeolites is an important key in the solid acid catalysis. CFI-II and CFI-III, which are needle crystals less than 2 μm in length, are small enough for higher activity of the isopropylation. On the other hand, CFI-I, which is large plate crystals (45 μm long and 10 μm wide), has the lowest activity among the CIT-5 zeolites. We suggest that the low activity is due to the low pore volume by the blockage of the channels, the small number of pore entrances in the large crystals, and to the low diffusivity of the reactant and products in the channels. The highest selectivity for 4,4′-DIPB obtained for CFI-I indicates the shape-selectivity of the CFI channels, and that the isomerization of 4,4′-DIPB at external acid sites reduces the selectivities in the isopropylation of BP over CFI-II and CFI-III.

4. Conclusion

CIT-5 zeolite, a 14-MR zeolite with CFI topology, worked as a shape-selective catalyst in the isopropylation of BP at moderate temperatures below 300 °C: the selectivities for 4,4′-DIPB were 50–60% in the bulk and encapsulated products. These results mean that the channels of CIT-5 zeolite can preferentially exclude the transition state of the bulky DIPB isomers from the channels, resulting in the selective formation of 4,4′-DIPB. However, the selectivity for 4,4′-DIPB over CIT-5 zeolite was lower than that over MOR. The CIT-5 channels may be too large for the selective formation of 4,4′-DIPB compared to MOR. Another difference between CIT-5 and MOR zeolites is the difference in the selectivities for 4,4′-DIPB in the encapsulated products at higher temperatures. The decrease in the selectivity for 4,4′-DIPB in the encapsulated products means that the isomerization of 4,4′-DIPB occurred at the external and internal acid sites of CIT-5 zeolite, however, no such a decrease in the selectivity for 4,4′-DIPB was observed for the MOR. These differences are due to the differences in the structures of these zeolites.

Shape-selective formation of 4,4′-DIPB over CIT-5 zeolite in this work is the first example of shape-selective catalysis over 14-MR zeolites. Further aspects of the influence of the shape-selective catalysis on the zeolite structures are being investigated. The details will be discussed in the near future.

Acknowledgements

A part of this work was financially supported by a Grant-in Aid for Scientific Research (B) 15350093 and 16310056, the Japan Society for the Promotion of Science (JSPS), and by Research Project under the Japan–Korea Basic Scientific Cooperation Program, JSPS and Korea Science and Engineering Foundation (KOSEF Grant no. F01-2004-000-10510-0).

References

[1] Y. Sugi, Y. Kubota, in: J.J. Spivey (Ed.), Catalysis, Specialist Periodical Report, vol. 13, Royal Soc. Chem., 1997, pp. 55–84 (Chapter 3).
[2] Y. Sugi, K. Komura, J.-H. Kim, J. Korean Ind. Eng. Chem. 17 (2006) 235.

[3] Y. Sugi, Y. Kubota, T. Hanaoka, T. Matsuzaki, Catal. Survey Jpn. 5 (2001) 43.
[4] T. Matsuzaki, Y. Sugi, T. Hanaoka, K. Takeuchi, H. Arakawa, T. Tokoro, G. Takeuchi, Chem. Express 4 (1989) 413.
[5] Y. Sugi, T. Matsuzaki, T. Hanaoka, Y. Kubota, J.-H. Kim, X. Tu, M. Matsumoto, Catal. Lett. 27 (1994) 315.
[6] Y. Sugi, S. Tawada, T. Sugimura, Y. Kubota, T. Hanaoka, T. Matsuzaki, K. Nakajima, K. Kunimori, Appl. Catal. A: Gen. 189 (1999) 251.
[7] G.S. Lee, J.J. Maj, S.C. Rocke, J.M. Garces, Catal. Lett. 2 (1989) 243.
[8] T. Matsuda, T. Urata, U. Saito, E. Kikuchi, Appl. Catal. A: Gen. 131 (1995) 215.
[9] C. Song, Compt. Rend. Acad. Sci., serie IIc: Chim. 3 (2000) 477.
[10] X.-W. Guo, X.-S. Wang, J.-P. Shen, C. Song, Catal. Today 93–95 (2004) 411.
[11] J. Horniakova, D. Mravec, J. Joffre, P. Moreau, J. Mol. Catal., A: Chem. 185 (2002) 249.
[12] Y. Sugi, Y. Kubota, A. Ito, H. Maekawa, R.K. Ahedi, S. Tawada, S. Watanabe, I. Toyama, C. Asaoka, H. Lee, J.-H. Kim, G. Seo, Stud. Surf. Sci. Catal. 154 (2004) 2228.
[13] H. Maekawa, A. Ito, H. Kawagoe, K. Komura, Y. Kubota, Y. Sugi, Bull. Chem. Soc. Jpn. 80 (2007) 215.
[14] M. Bandyopadhyay, R. Bandyopadhyay, S. Tawada, Y. Kubota, Y. Sugi, Appl. Catal. A: Gen. 225 (2002) 51.
[15] S.K. Saha, S.B. Waghmode, H. Maekawa, K. Komura, Y. Kubota, Y. Sugi, Y. Oumi, T. Sano, Micropor. Mesopor. Mater. 81 (2005) 289.
[16] S.K. Saha, H. Maekawa, S.B. Waghmode, S.A.R. Mulla, K. Komura, Y. Kubota, Y. Sugi, -S.J. Cho, Mater. Trans. 46 (2005) 2659.
[17] H. Maekawa, S.K. Saha, S.A.R. Mulla, S.B. Waghmode, K. Komura, Y. Kubota, Y. Sugi, J. Mol. Catal. A: Chem. 263 (2006) 238.
[18] R.K. Ahedi, S. Tawada, Y. Kubota, Y. Sugi, J.-H. Kim, J. Mol. Catal. A: Chem. 197 (2003) 133.
[19] IZA Structure Commission: http://www.iza-structure.org/databases/.
[20] P. Wagner, M. Yoshikawa, K. Tsuji, M.E. Davis, P. Wagner, M. Lovallo, M. Tsapatsis, Chem. Commun. (1997) 2179.
[21] M. Yoshikawa, P. Wagner, M. Lovallo, K. Tsuji, T. Takewaki, C.-Y. Chen, L.W. Beck, C. Jones, M. Tsapatsis, S.I. Zones, M.E. Davis, J. Phys. Chem. B 102 (1998) 7139.
[22] Y. Kubota, S. Tawada, K. Nakagawa, C. Naitoh, N. Sugimoto, Y. Fukushima, T. Hanaoka, Y. Imada, Y. Sugi, Micropor. Mesopor. Mater. 37 (2000) 291.
[23] M.K. Rubin, U.S. patent, 5,164,169 (1992).
[24] R.F. Lobo, M. Tsapatsis, C.C. Freyhardt, S. Khodabandeh, P. Wagner, C.-Y. Chen, K.J. Balkus Jr., S.I. Zones, M.E. Davis, J. Am. Chem. Soc. 119 (1997) 8474.
[25] A. Burton, S. Elomari, C.-Y. Chen, R.C. Medrud, -I.Y. Chan, L.M. Bull, C. Kibby, T.V. Harris, S.I. Zones, E.S. Vittoratos, Chem. Eur. J. 9 (2003) 5737.
[26] Unpublished results.